

Operational Use of Near-Real-Time Sea Surface Directional Wave Spectra Generated from NOAA Scanning Radar Altimeter Range Measurements

Edward J. Walsh, Principal Investigator
Code 614.6, NASA Goddard Space Flight Center, Greenbelt, MD 20771
office 303-497-6357
cell 303-579-7811
edward.walsh@noaa.gov

December 12, 2008 - Mid-Year Report

ProSensing has settled on a name for the instrument they built as an operational replacement for the NASA Scanning Radar Altimeter (SRA). They have called it the Wide Swath Radar Altimeter (WSRA). This is a very appropriate name since the NOAA WSRA produces a wide swath similar to the NASA SRA, but not by scanning a narrow beam as the SRA did. And the acronym incorporates the heritage of the NASA system. Earlier reports have dealt with the interactions with the JHT points of contact in developing the details of the display programs I supplied to Jose Salazar. Jose implemented and tested them on the JHT server and they were ready at the start of the 2008 hurricane season to process WSRA data and display it on the JHT computers or in NAWIPS.

The plan was to process WSRA data on the aircraft during the flights and transfer it to a server at the NOAA Aircraft Operations Center (AOC) in Tampa, which would relay the files to the JHT server to display for the forecasters. John Hill (AOC) was too busy before the start of the 2008 season implementing and verifying the performance of a new aircraft data system to establish the WSRA data link. When he finally was able to implement the data link, Brian Maher (NHC) indicated that the TPC/NHC firewall would have to be modified to allow the AOC server access. It was unanticipated that there would be security concerns about allowing access from the NOAA AOC server, another NOAA computer situated on the secured facility of MacDill Air Force Base. If that impasse remains unresolved as the 2009 hurricane season approaches, it may be possible to reverse the roles, with John Hill placing the WSRA data in a public area and the JHT server going to that site in search of it rather than having it delivered directly.

Had the firewall problem not preempted it, the end-to-end data transfer and display functions could have been tested. But the WSRA still would not have been operational because Ivan PopStefanija of ProSensing made the prudent decision to record all the raw data during the 2008 season to be able to identify and correct any unanticipated problems in the hardware. The WSRA collected data during flights into Hurricanes Fay, Gustav and Ike. I will use the second flight into Ike for purposes of illustration.

At 2,400 m altitude the WSRA recorded 1 Giga Byte of raw data every 30 s. In the 3.5 hours of data acquisition during the second flight into Hurricane Ike on 11 September 2008, the WSRA recorded about 400 GB. The thin line in the left panel of Figure 1 shows the track of N43RF carrying the WSRA with the thick portions of the track indicating where the WSRA acquired data. The thick lines in the right panel indicate the temporal acquisition intervals. Because of the huge data volume, the WSRA was not operated during the transits to and from Ike and the system could not be operated continuously while in the vicinity of Ike. But the coverage within Ike was still extensive with all quadrants of the hurricane being sampled.

The original plan for the 2008 season was for me to go on the flights along with the ProSensing WSRA operator, either Ivan PopStefanija or Chad Baldi, intermittently process data with my backend analysis programs, and transmit it through the AOC server to the JHT server for display. But operational constraints by AOC allocated only one seat to the WSRA. I did not go on the only flight where a second WSRA seat could have been made available because the data link to JHT had not been established.

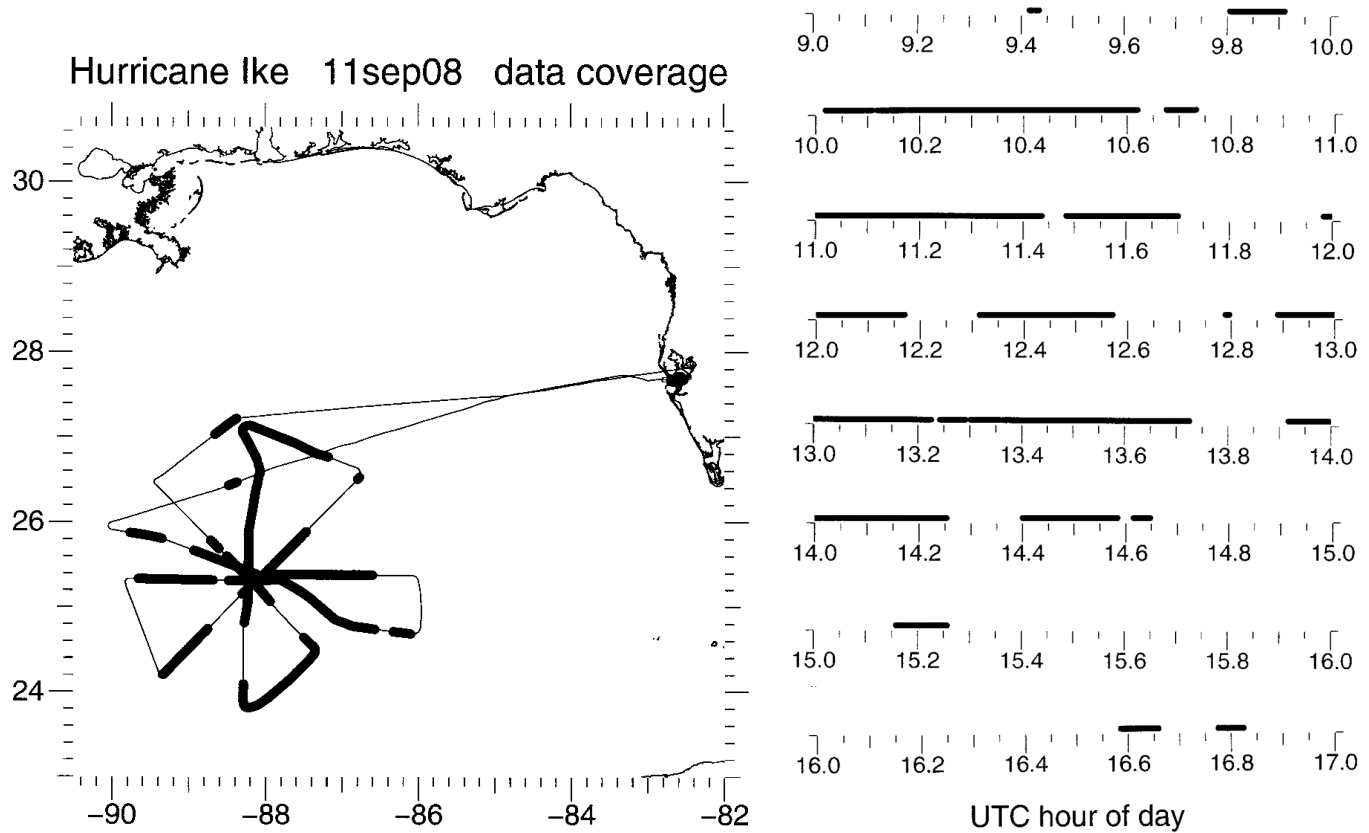


Figure 1. N43RF track (thin line) and WSRA data acquisition intervals (thick lines).

I will briefly describe each of four WSRA data products that could be of great value.

1. **Directional wave spectra** measurement for initializing, verifying and improving the performance of numerical wave models and for providing wave field parameters such as the radius of 12' seas.
2. **Storm surge** measurement for landfalling hurricanes to verify and improve the performance of the numerical storm surge models and help emergency managers allocate post storm resources.
3. **Rain rate** measurement with a higher sensitivity to light rain than the SFMR.
4. **Sea surface mean square slope** (small scale roughness) measurement to aid air-sea interaction studies.

DIRECTIONAL WAVE SPECTRA

Directional wave spectra from the NASA SRA have helped investigate the air-sea transfers in hurricanes (Black et al. 2007) and assess the performance of the WaveWatch III (WW3) numerical wave model (Moon et al. 2003) and given insight into how to improve them (Fan et al. 2009).

- Black, P. G., E. A. D'Asaro, W. M. Drennan, J. R. French, P. P. Niiler, T. B. Sanford, E. J. Terrill, E. J. Walsh, J. A. Zhang, 2007: Air-sea exchange in hurricanes: synthesis of observations from the Coupled Boundary Layer Air-Sea Transfer experiment, *Bull. Am. Met. Soc.*, **88**, 357-374.
- Fan, Y., I. Ginis, T. Hara, C. W. Wright and E. J. Walsh, 2009: Numerical simulations and observations of surface wave fields under an extreme tropical cyclone, in preparation.
- Moon, I.-J., I. Ginis, T. Hara, H. L. Tolman, C. W. Wright and E. J. Walsh, 2003: Numerical simulation of sea surface directional wave spectra under hurricane wind forcing. *J. Phys. Oceanogr.*, **33**, 1680-1706.

Figure 2 shows a figure from Fan et al. (2009) which compares WW3 wave parameters with Hurricane Ivan observations by SRA on 14 September 2004 in the Gulf of Mexico at approximately the same location as Hurricane Ike in Figure 1. WW3 wave parameters were generated using old and new flux parameterizations as well as a coupled mode, which produced the best agreement with the SRA measurements. A disparity between model and observations occurred during the six eye penetrations (approximately spectrum numbers 30, 150, 270, 350, 460, and 565) where WW3 indicated a sharp drop in the Significant Wave Height in the eye and the SRA did not. Subsequent simulations suggested that a larger wind inflow angle than in the WW3 wind field probably caused the higher observed wave height in the eye.

The top panel of Figure 3 shows a blow-up of the track of N43RF in the vicinity of Hurricane Ike with the location of Buoy 42001 indicated. The dominant waves in the vicinity of a hurricane are generally swell originating in the vicinity of the radius of maximum wind (RMW). The bottom right panel of Figure 3 shows the spatial relationship between the track of Hurricane Ike and the WSRa at Buoy 42001. The bottom left panel shows gray-scale coded wave topography measured by the WSRa at Buoy 42001. Swell generated in the vicinity of the RMW would be propagating toward the west at Buoy 42001 and that is apparent in the WSRa wave topography. The local wind at Buoy 42001 generated by Ike would be toward the SSW and the wind sea it generated is also apparent in the wave topography.

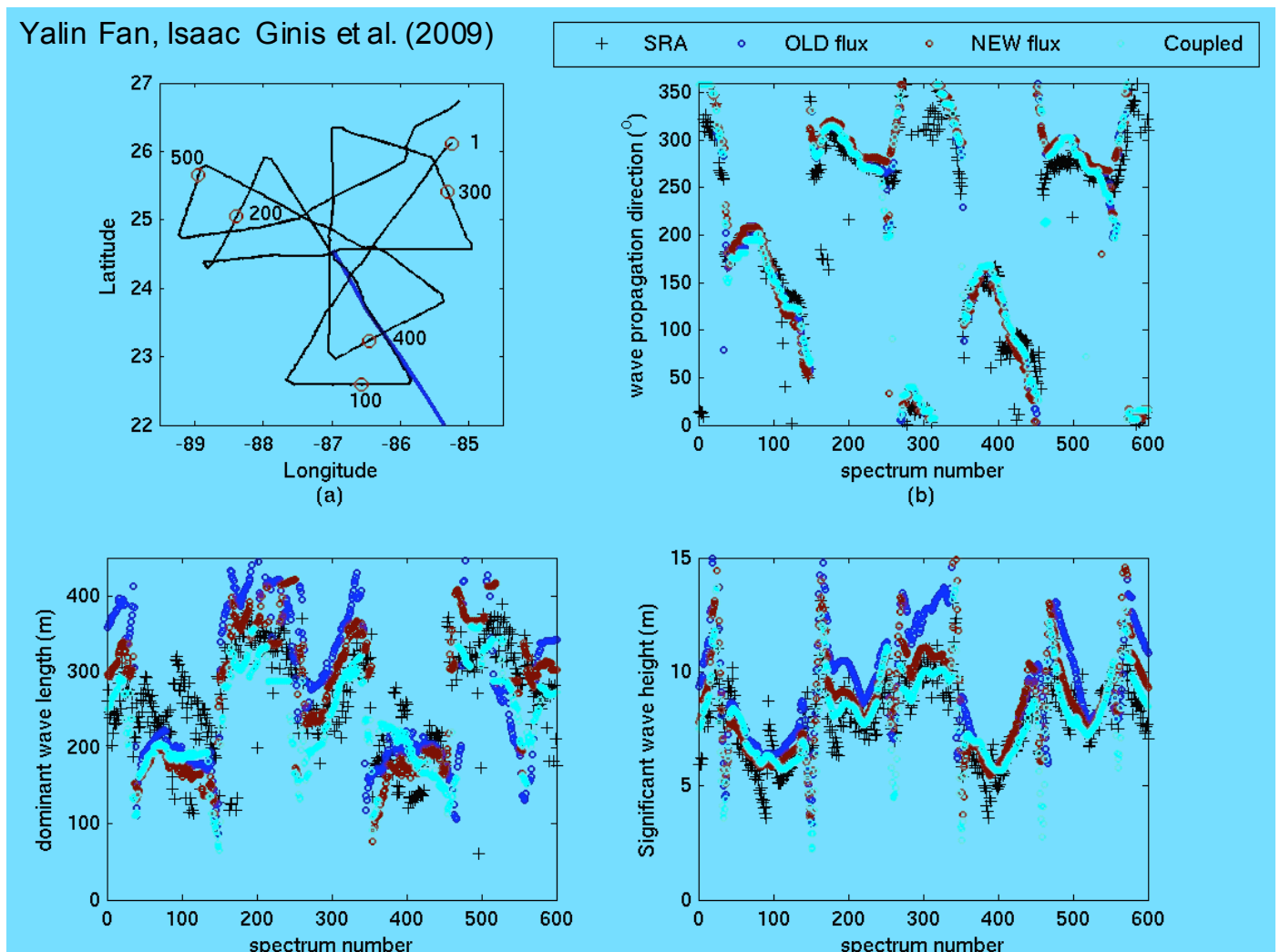
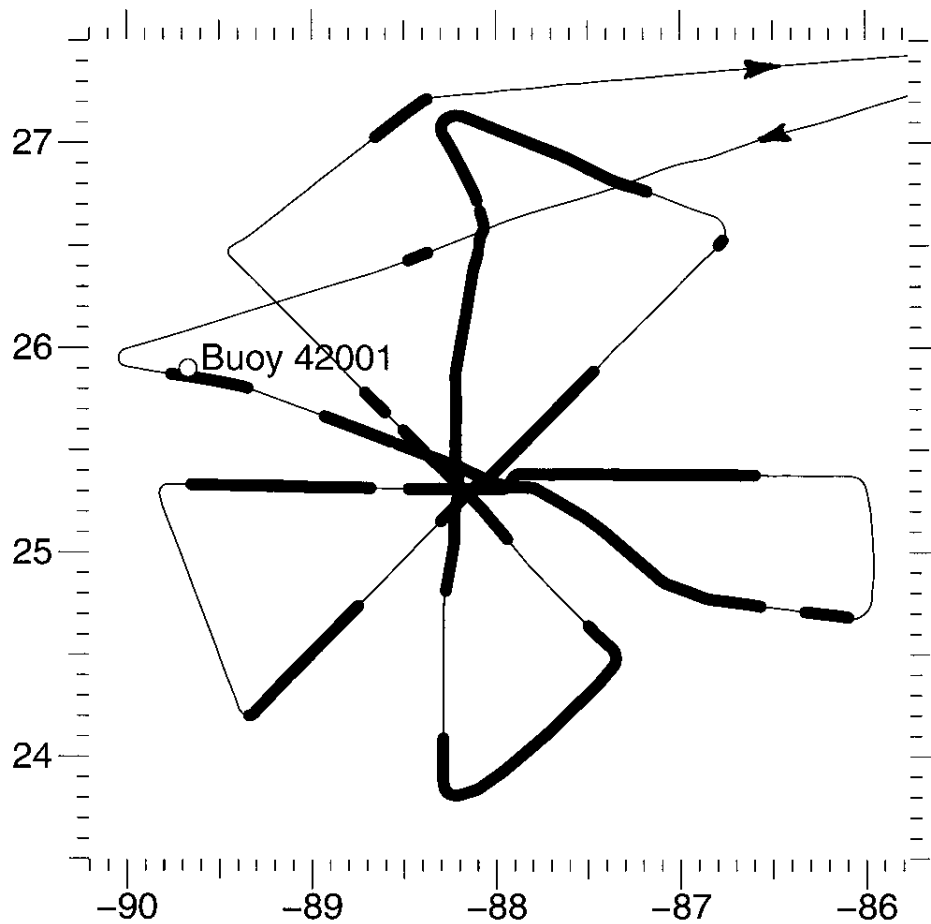


Figure 2. SRA observations and WW3 results comparison for experiments A, B and C for Sept. 14-15 flight. (a) Blue is hurricane track. Black is flight track, and the red circle and number shows the spectrum number along the flight. (b) Wave propagation direction relative to true north rotating clockwise, (c) dominant wave length, and (d) significant wave height comparison between SRA measurements and model results from Exp. A, B and C. (This is Figure 6 from Fan et al. 2009.)

Hurricane Ike 11sep08 data coverage



System : 0 (0.6940, 0.3508)

System : 1 (-84.2539, 21.2034)

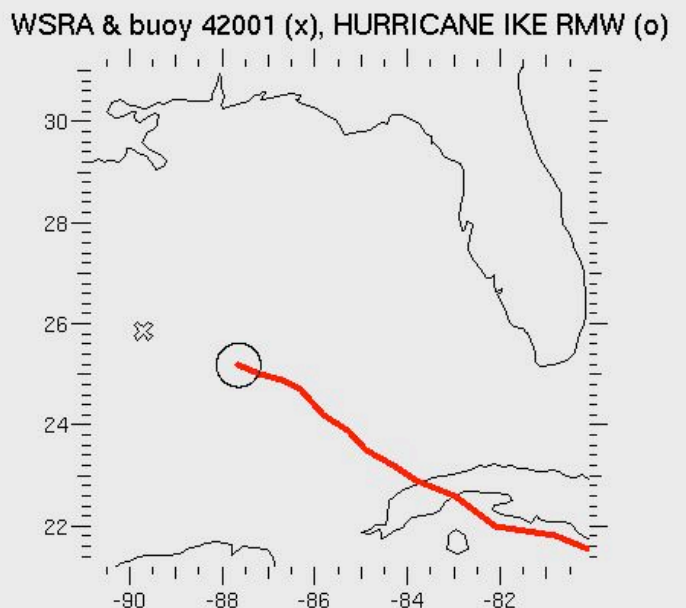
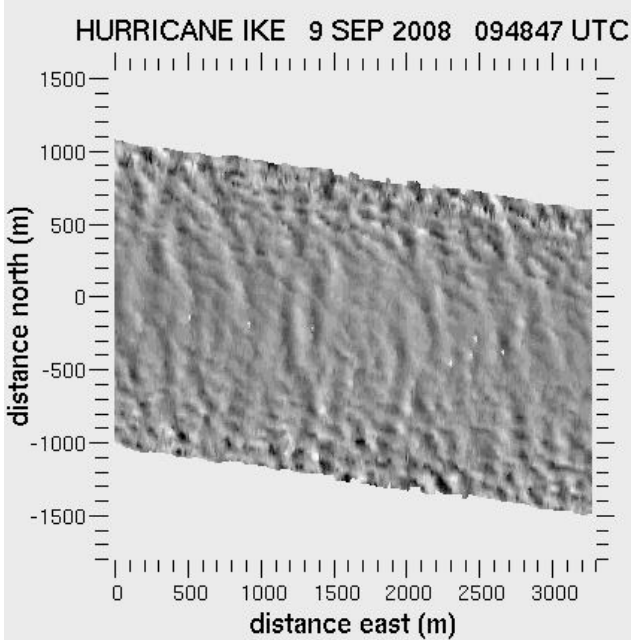


Figure 3. WSRA data coverage in the vicinity of Hurricane Ike (thick segments, top panel). WSRA gray-scale coded wave topography at Buoy 42001 (bottom left panel, mislabeled as 9 instead of 11 SEP). Bottom right panel indicates Hurricane Ike track (red) and its RMW (circle) with the location of the WSRA and Buoy 42001 indicated (X).

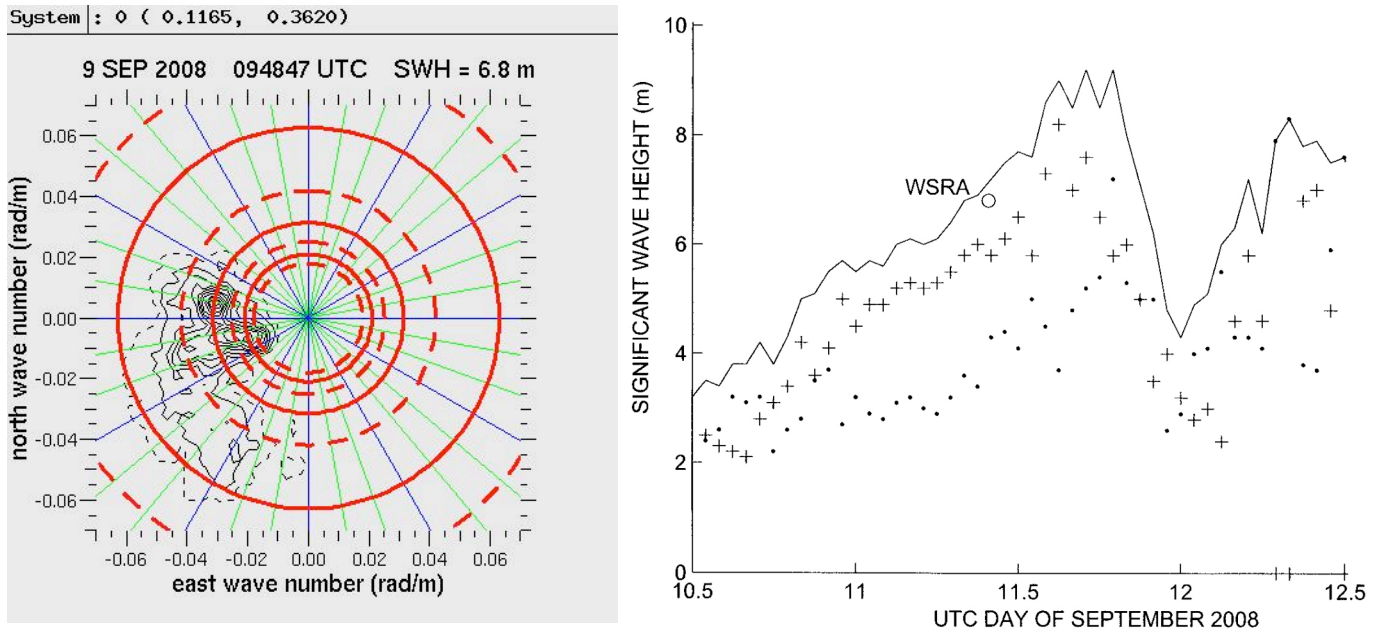


Figure 4. Left panel - directional wave spectrum generated from the wave topography in Figure 3. The nine solid contours are at equal intervals from 0.9 to 0.1 of the peak spectral density. The dashed contour is at the 5% level. The three solid red circles indicate wavelengths of 100, 200 and 300 m (outer to inner) and the four dashed circles indicate wavelengths of 75, 150, 250 and 350 m. Right panel - Buoy 42001 wave height variation, total(-), swell(+), sea(.), and the WSRA (o) value.

The left panel of Figure 4 shows the directional wave spectrum generated from the wave topography in Figure 3. The spectrum indicates westward propagating waves of 200 to 300 m wavelength and a secondary wave field of about 130 m propagating toward 210°. The right panel of Figure 4 shows the temporal variation of the wave height at Buoy 42001 over a two day period. The dip in the wave height at 0000 UTC on 12 September was because Buoy 42001 was within the RMW as Hurricane Ike passed by. The buoy data indicate that the swell component at the time of the WSRA measurement was about 6 m and the sea component was about 4 m.

The WSRA value is slightly lower than the buoy wave height but that is quite reasonable considering that the 3 km along-track distance used in the WSRA estimate interrogated only 10 to 15 wavelengths of the swell. Wave trains vary spatially, as is apparent in Figure 3, and the WSRA data span represents less than 3 minutes of the waves passing by Buoy 42001 during its 20 minute averaging time to produce each hourly value of wave height.

STORM SURGE

Over the years, hurricane track and intensity forecasts and storm surge models and the digital terrain and bathymetry data they depend on have improved significantly. Strides have also been made in knowledge of the detailed variation of the surface wind field driving the surge. The area of least improvement has been in obtaining detailed data on the temporal/spatial evolution of the mound of water the hurricane wind and waves push against the shore to evaluate the performance of the numerical models. Tide gages in the vicinity of the landfall are frequently destroyed by the surge. Survey crews dispatched after the event provide no temporal information and only indirect indications of the maximum water level over land.

SRA measurements on 26 August 1998 during the landfall of Hurricane Bonnie, whose surge was less than 2 m, demonstrated that, despite a 160 m variation in aircraft altitude, an 11.5 m variation in the elevation of the mean sea surface relative to the ellipsoid over the flight track, and the tidal variation over the 5 hour data

acquisition interval, a wide swath radar altimeter supported by a survey-quality Global Positioning System (GPS) aircraft trajectory could produce targeted measurements of storm surge that would provide an absolute standard for assessing the accuracy of numerical storm surge models and providing emergency managers with observational guidance on the deployment of post-storm resources.

The top panels of Figure 5 superimpose on the SLOSH and North Carolina State University (NCSU) storm surge contours the aircraft tracks which began near Cape Lookout and passed through Onslow Bay with a time separation of about four hours. Two things stand out. First, although the orientation of the surge elevation contours in Onslow Bay for SLOSH rotates clockwise over the 4 hour period, they remain roughly 18° counterclockwise from the NCSU contours, which also rotate. Second, the middle panels of Figure 5 indicate the NCSU model water level west of Cape Fear that is about one meter lower than SLOSH with the SRA observations being between the two models. With few exceptions, the SRA surge values in Figure 5 cluster tightly about their mean trend. The gap in the SRA data in the region between 80 and 120 km north of 34°N in the left panel and in the right panel between -150 and -130 km is due to land contamination.

Both models indicate about the same peak surge, but NCSU suggests that the maximum would occur further north than SLOSH at both observation times. The SRA indicates that the peak of the surge was actually south of the SLOSH position at both observation times. The bottom panel of Figure 5 suggests that much of the difference in the surge values of the models may have been caused by the different tracks they used for Hurricane Bonnie. The SLOSH track (dashes) was determined by a spline fit through the NHC 6-hour interval Best Track storm positions (X). NCSU used the eye locations (dots) at two hour intervals issued in the NHC advisories during landfall. There was not much difference in the tracks prior to 1500 UTC, but then the NHC 2-hour advisories moved Bonnie forward too rapidly in addition to diverting it toward the west. The NHC 2-hour advisories placed Bonnie at 33.7°N at 1900 UTC while the SRA aircraft suggested that it didn't reach that latitude until 2000 UTC and the Best Track indicated 2100 UTC, a two-hour spread. The NHC 2-hour advisories placed Bonnie at 34°N at 2100 UTC while the SRA aircraft suggested that it didn't reach that latitude until about 2300 UTC and the Best Track indicated 2400 UTC, a three-hour spread. In addition to the aircraft indicating a forward speed for Bonnie between that used by SLOSH and NCSU, two of the aircraft eye locations were between the tracks used by SLOSH and NCSU. That might also help explain why the SRA surge was sometimes between the two models.

Dashed radials extend from the 2100 UTC eye locations on the two tracks to Springmaid Pier and to the middle on Onslow Bay. Arrows drawn from the Springmaid Pier and Onslow Bay locations at right angles to the dashed radials provide a simple indication of differences in the local downwind direction caused by the track differences. In the middle of Onslow Bay the downwind direction for NCSU would have been rotated 30° clockwise from SLOSH, which was greater than the 18° clockwise rotation in the surge elevation contours in evidence in the top panels. At Springmaid Pier the NCSU downwind direction would have been 21° closer to being perpendicular to the shoreline and presumably more effective in producing a depressed water surface. Halfway between Springmaid Pier and Cape Fear, the NCSU downwind direction would have been directly offshore while SLOSH would have been 33° off the normal to the shoreline.

An actuated GPS antenna mount was developed by NASA after the Hurricane Bonnie landfall flight to maintain a zenith orientation during the large roll maneuvers the NOAA aircraft employ. It has been transferred to NOAA for use with the WSRA so the quality of the GPS trajectories should be even better than for Hurricane Bonnie. The WSRA, with improved data quality and less susceptibility to rain attenuation, will be able to produce targeted measurements of storm surge that would provide an absolute standard for assessing the accuracy of numerical storm surge models and providing emergency managers with timely information on the actual surge.

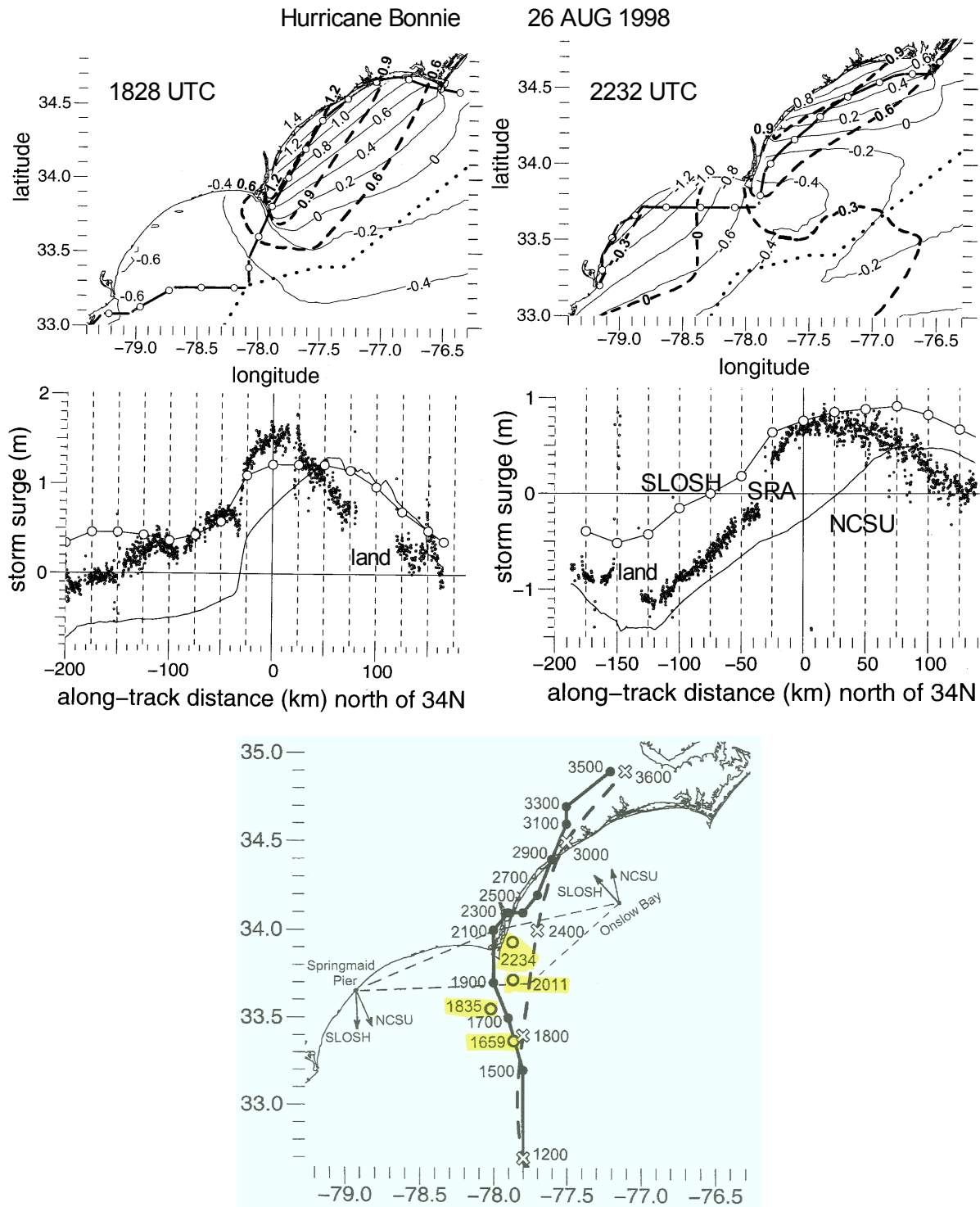


Figure 5. Circles (top panels) identify positions along the aircraft track spaced at 25 km intervals along the flight line relative to passing 34°N. The thin lines indicate the NCSU storm surge contours when the aircraft passed through 34°N at the times indicated. The thick dashed lines indicate the SLOSH storm surge contours. Dots indicate a piecewise linear approximation of the western edge of the Gulf Stream. In the middle panels, dots indicate SRA storm surge values along the flight track. The curve without the circles indicates the NCSU surge values along the flight track. SLOSH surge values are indicated by the circles connected by line segments. The bottom panel shows NHC Best Track storm positions (X) and the eye locations (dots) from NHC advisories issued during landfall with time incrementing from 0000 UTC on 26 August 1998. The four circles indicate eye locations recorded in the N43RF Flight Director's log (Barry Damiano, NOAA/AOC, personal communication, 2007) from 1659, 1835, 2011 and 2234 eye penetrations.

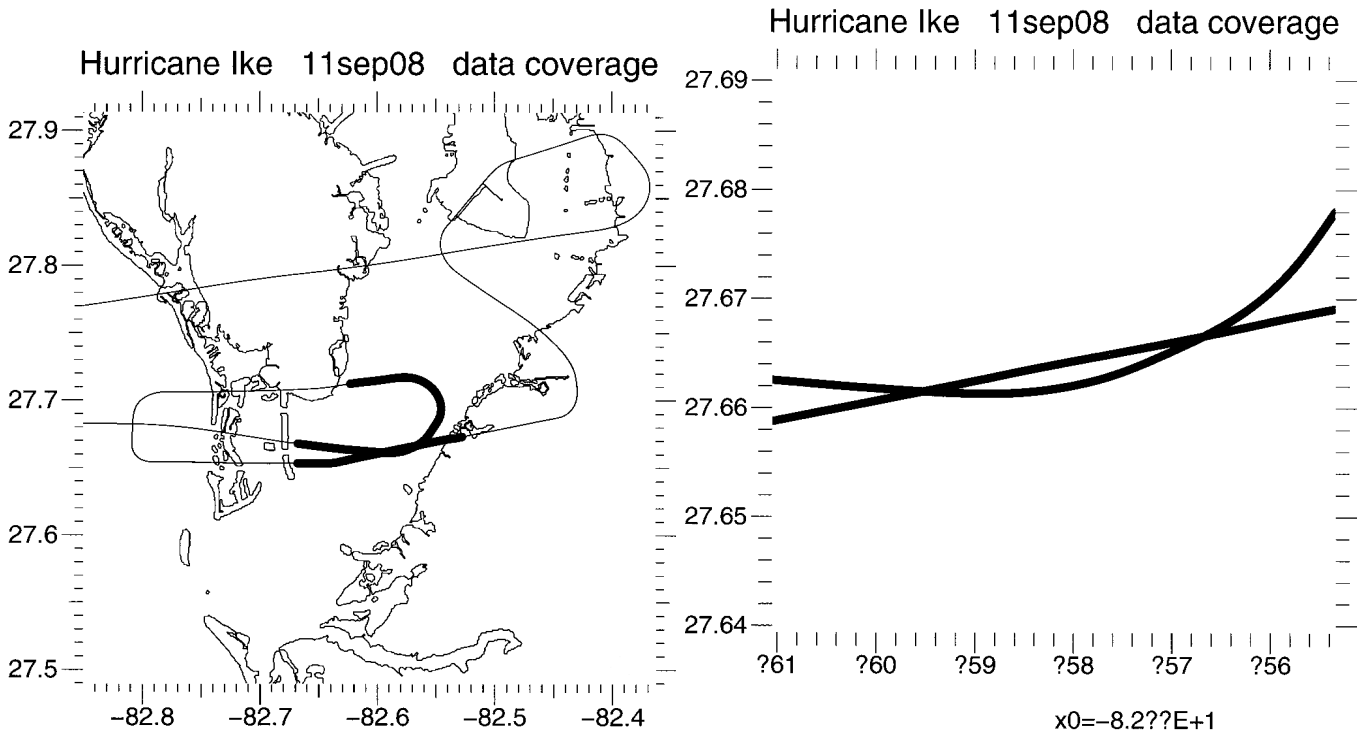


Figure 6. N43RF flight track at the beginning and end of the Hurricane Ike flight on 11 September 2008 with the WSR data acquisition intervals indicated by the thick lines (left panel) and a blow-up (right panel).

Figure 6 indicates the WSR data acquisition intervals during two passes through Tampa Bay at the end of the second flight into Hurricane Ike. The water level in Tampa Bay varies very gradually and there are several tide gauges in the bay that can be used in an absolute calibration of the WSR range measurements as it returns from a storm surge measuring flight, in addition to any tide gauges that might be in the vicinity of the landfall itself. There is also a 300 m by 300 m area on the ramp near the AOC hangar where NASA GSFC performed a high density survey that could be flown over prior to landing. The data indicated in Figure 6 were acquired to begin the absolute range calibration process. Jason Woolard of the NOAA/NOS National Geodetic Survey Remote Sensing Division produced a GPS aircraft trajectory for the subset of data indicated in Figure 6 that was accurate to a few cm. But those WSR data have not been reduced yet for reasons to be discussed at the end of this report.

RAIN RATE

Figure 7 indicates the situation for the NASA SRA entering a region of rain. At its 36 GHz operating frequency the SRA experienced a round trip signal attenuation of 0.86 dB for each mm/hr of rain rate. Figure 8 shows data from a SRA flight into Hurricane Humberto on 24 September 2001. To first order, the power backscattered from the sea near nadir is Gaussian distributed in incidence angle with its peak value inversely proportional to mean square slope (mss) and its falloff with incidence angle also inversely proportional to mss. When the log of the backscattered power is plotted against the square of the incidence angle tangent, the result is a straight line to first order.

The left panel of Figure 8 shows data from two intervals when it was not raining. The far left plot shows 5 contiguous, nonoverlapping 10-s averages when the wind speed was 6 m/s. The second plot also shows 5 10-s averages, contiguous and nonoverlapping, when the wind speed was 12 m/s.

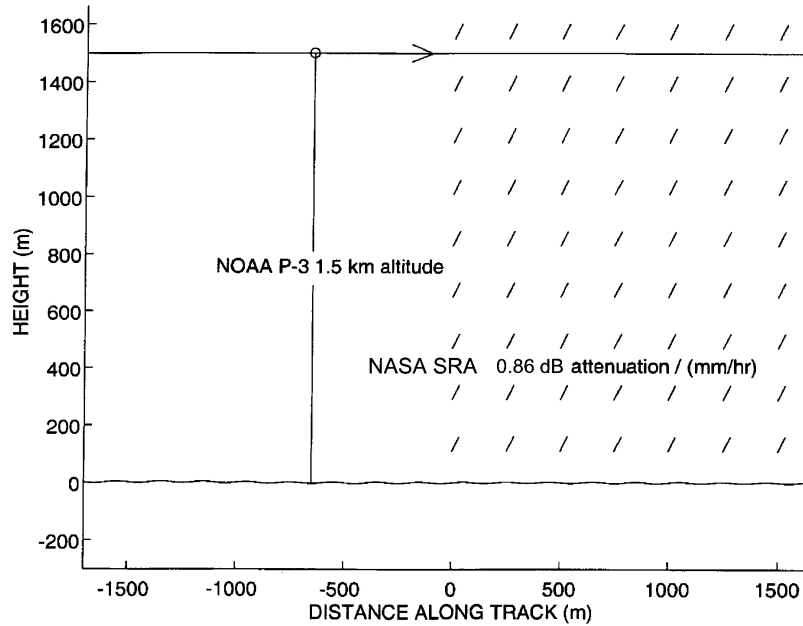


Figure 7. Schematic view of SRA entering a region of rain.

The data points in each of the 5 averages and the straight lines least squares fitted to them are nearly identical. The lower wind speed case has a higher nadir power and a faster falloff with incidence angle while the higher wind speed has a lower nadir power and a slower falloff. The right panel of Figure 8 shows 100 s of data in 10 contiguous, nonoverlapping 10 s averages during which the rain increased from 3 to 9 mm/hr over 50 s and then decreased from 9 to 3 mm/hr over the next 50 s. The aircraft was at 1800 m altitude during the data acquisition shown in Figure 8 and the SRA experienced a 1 dB attenuation for each mm/hr rain rate. The mss may change when the aircraft enters a region of rain and that also affects the backscattered power but it is possible to determine that by the falloff with incidence angle and normalize all nadir powers to a constant mss. Then any decrease below the maximum value is due to rain attenuation.

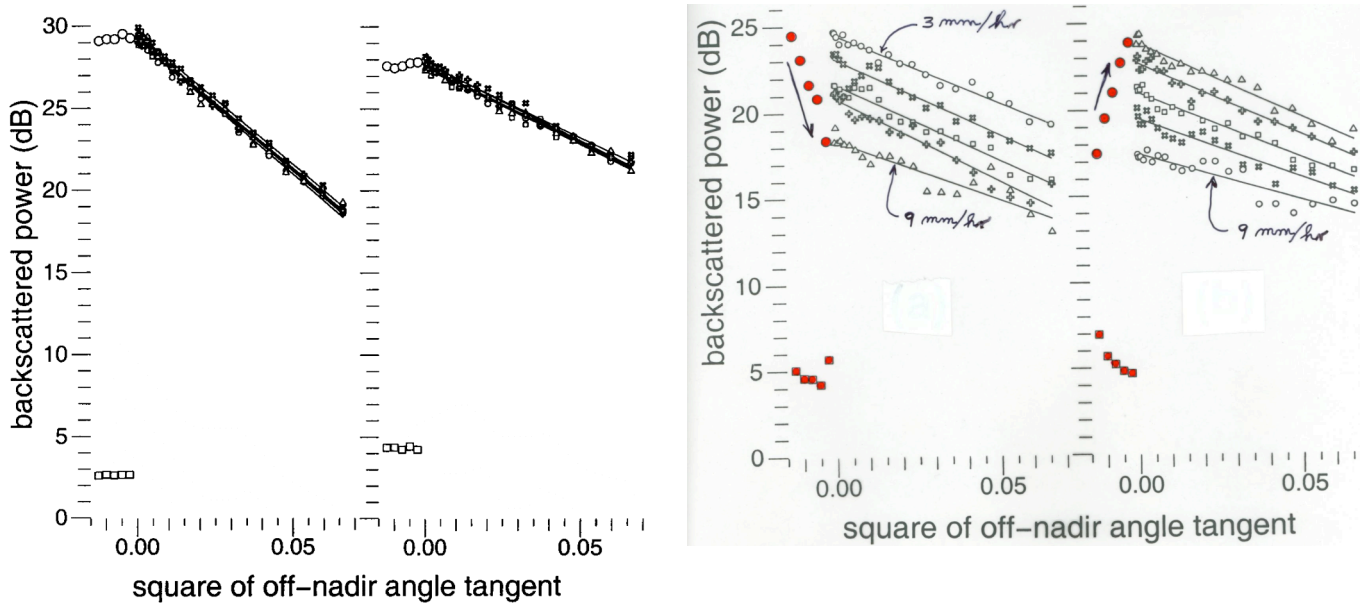


Figure 8. SRA backscattered power variation with incidence angle at 1800 m altitude for 5 nonoverlapping, contiguous averages of 10-s in the absence of rain for wind speed of 6 m/s (far left) and 12 m/s (2nd from left), and for rain increasing from 3 to 9 mm/hr (3rd from left), then decreasing back from 9 to 3 mm/hr.

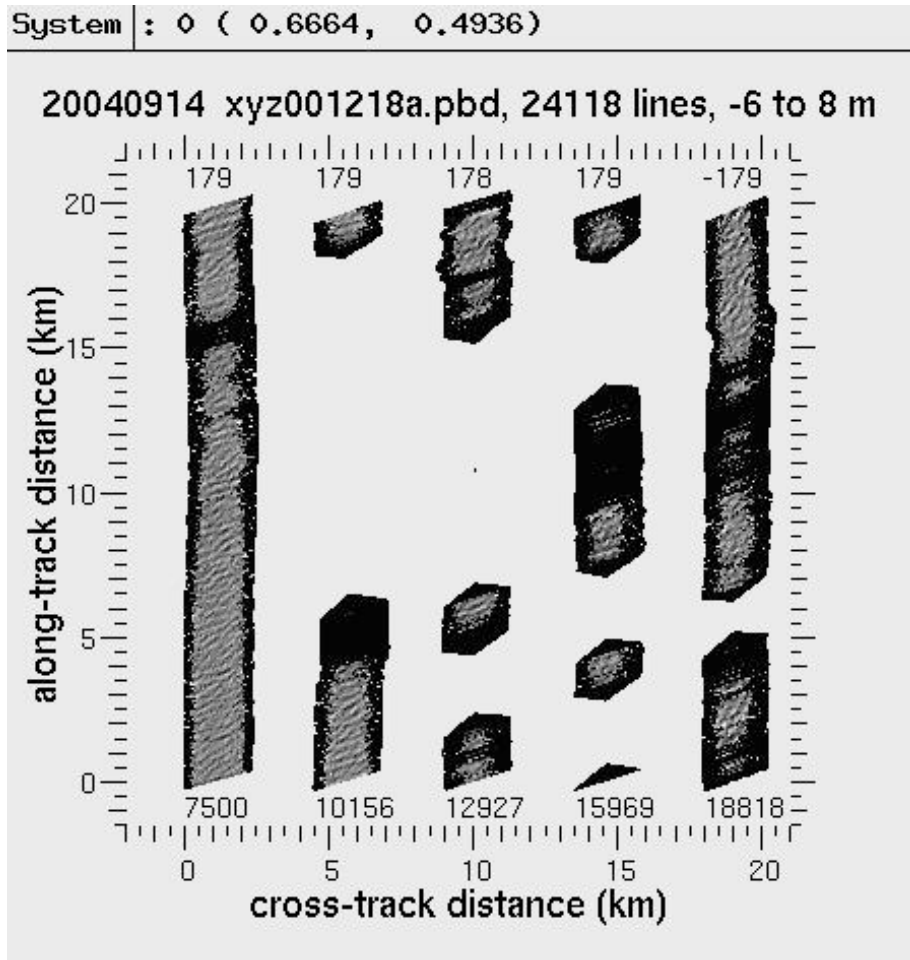


Figure 9. SRA gray-scale coded wave topography in Hurricane Ivan on 14 September 2004.

The negative aspect of the SRA high sensitivity to rain rate was that its signal was frequently totally attenuated by rain. Figure 9 shows 100 km of SRA wave topography broken into 5 20-km segments when the aircraft was north of Hurricane Ivan on 14 September 2004 heading south toward the eye at 3 km altitude. The SRA signal was total attenuated about half the time. The WSRA uses pulse compression and operates at 16 GHz instead of 36 GHz so it will rarely have data dropouts. The WSRA lower frequency is 6 times less sensitive to rain attenuation than SRA, but it is still 8 times more sensitive than the SFMR, whose frequency is even lower and uses the same absorption technique to determine rain rate.

MSS

Because the WSRA has an order of magnitude higher pulse repetition frequency than the SRA and averages the extra pulses to improve the quality of the wave topography and reduce the random fluctuations in the power measurements, its determination of mss will be significantly better than for the SRA. Higher quality, registered maps of wave topography and backscattered power offer the possibility of being able to examine surface roughness variations over the dominant waves in a hurricane. It might be possible to investigate whether there is more flow separation (lower mss) on the lee side of waves in the right front quadrant of a hurricane where the wind is blowing perpendicular to the dominant wave crests than in the left front quadrant where the wind is blowing parallel to the dominant wave crests.

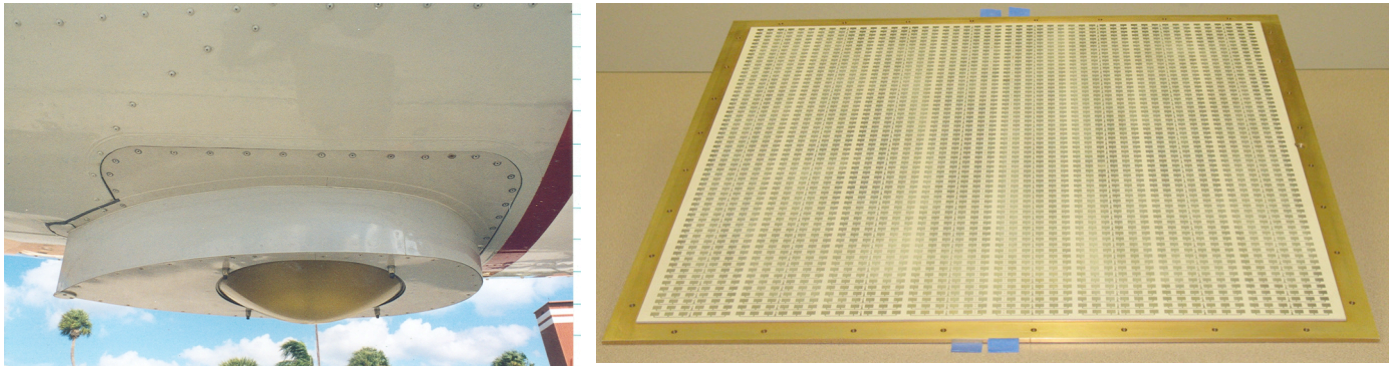


Figure 10. SRA dielectric lens antenna (left) and WSRA slotted waveguide antenna (right).

Status of WSRA and data analysis

I want to point out the remarkable accomplishment of ProSensing. The NASA SRA was built at a cost of \$1,000,000 fifteen years ago. It was funded at \$250 K/year for four years and that did not include several man years of civil service time. The SRA transmitted a short pulse (6 ns) of 1.5 KW peak power and measured its time of flight. The Klystron used to achieve that power level cost \$300 K by itself.

ProSensing was given \$300 K by the NOAA SBIR program to build the entire WSRA. And the WSRA is two orders of magnitude more complex than the SRA. The WSRA transmits a long, chirped pulse so that it can operate with a peak power of only 10 W. At 3 km height the range extent of the WSRA pulse would be 2900 m whereas the SRA pulse range extent was only 0.9 m. The result is that the WSRA has better signal level than the SRA even though its peak transmitted power is two orders of magnitude lower.

The left panel of Figure 10 shows the dielectric lens the SRA used to form a narrow beam (1° 2-way) which was scanned mechanically by a rotating mirror. The WSRA sequentially transmits its chirped pulse on each of 62 slotted wave guide elements (right panel) which produce narrow beams in the along-track direction, but fan beams in the cross-track direction. Those 62 return pulses are dechirped to provide range resolution and then combined coherently with various phase shifts to produce 80 narrow beams in the cross-track direction.

ProSensing leveraged an antenna design grant from UMass and some hardware donated from a DARPA project that was terminated after Phase 1 to be able to complete the WSRA with the funds available from the NOAA SBIR program, but all their funding has long since been expended.

There appears to be a hardware sequencing problem which is causing either the range quantization or the beam angles to deviate from their nominal values. I was able to produce the results shown in Figures 3 and 4 by using a range resolution other than the nominal value, but the problem needs to be identified and corrected before the data can be routinely processed. Since all the raw data was recorded, the problem is resolvable. I am trying to assist Ivan PopStefanija of ProSensing with the raw data issues, but he is working in a background mode because of the need to focus on funded projects.

The Physical Sciences Division of the NOAA Earth System Research Lab, where I am assigned in Boulder, is assuming ownership of the WSRA, but there is not yet a line item in the NOAA budget for it. The WSRA is a remarkable instrument, but it is critical that the ProSensing JHT proposal be funded as soon as possible to complete its transition to operational status.